NASA's Deep-Space Telecommunications Road Map

C. D. Edwards, Jr.,[1] C. T. Stelzried,[1] L. J. Deutsch,[2] and L. Swanson[1]

With the advent of faster, cheaper planetary missions, the coming decade promises a significant growth in the number of missions that will be simultaneously supported by NASA's Deep Space Network (DSN). In addition, new types of missions will stretch our deep-space communications capabilities. Ambitious outer-planet missions, with extremely tenuous communications links due to their great distances, and data-intensive orbiter or in situ missions incorporating high-bandwidth science instruments will demand improved telecommunications capabilities. Ultimately, our ability to create a virtual presence throughout the solar system will be directly linked to our overall deep-space telecommunications capacity. The Telecommunications and Mission Operations Directorate (TMOD) at the Jet Propulsion Laboratory, which operates NASA's Deep Space Network, has developed a road map for deep-space telecommunications through the year 2010 that meets these challenges. Key aspects of this road map are: (1) a move to efficient, standard communications services; (2) development of an end-to-end flight–ground communications architecture and coordination of flight and ground technology developments; and (3) rapid infusion of Ka-band (32-GHz) and optical communications technologies into the DSN and into future spacecraft. This article presents this road map, describes how it supports an increasing mission set while also providing significantly increased science data return, summarizes the current state of key Ka-band and optical communications technologies, and identifies critical path items in terms of technology developments, demonstrations, and mission users.

I. Introduction

One of the primary goals identified within NASA's most recent strategic plan is "to establish a virtual presence throughout the solar system" [7]. The fidelity of this virtual presence will in large part be defined by the communications bandwidth that we can provide between our robotic spacecraft and the scientists, engineers, and public who interact with them here from Earth. Consistent with this, the National Research Council recently identified "wideband, high data-rate communications over planetary distances" as one of six key technologies with the potential to "lower the cost and improve the performance of existing space activities and enable new ones" [8]. The Telecommunications and Mission Operations Directorate (TMOD) recently carried out a study to examine our deep-space communications capability in a rigorous, quantitative way and to identify the most cost-effective options for future growth.

[1] TMOD Technology Program Office.

[2] Advanced Flight Systems Program Office.

Section II of this article describes the challenge TMOD faces as we move to an era of far more frequent launches. Section III then will present TMOD's strategy for responding to this challenge. In particular, we will focus on how TMOD is applying new technology developments in Ka-band (32-GHz) and optical communications to provide extremely cost-effective growth in our deep-space communications capability. Finally, in Section IV, we will summarize what we have learned in this study and what recommendations we are making regarding the future of deep-space communications.

II. Telecommunications Challenges

One of the great dividends of the "faster, better, cheaper" NASA is the agency's ability to launch far more frequent new missions. We have successfully evolved in a few short years from an era of infrequent "flagship" missions to frequently launched missions and multimission programs such as Discovery, Mars, and Outer Planets. Based on a conservative forecast of future missions, TMOD anticipates a significant increase in the number of missions supported, from a current level of roughly 25 simultaneous missions up to roughly 35 simultaneous missions in 5 years. (A more aggressive forecast, based on the NASA Administrator's goal of a launch every month, would lead to over 50 simultaneous missions.) This increasing mission set will stress the capacity of NASA's Deep Space Network (DSN).

In addition to the sheer number of missions, the types of missions NASA will fly also will stretch our deep-space communications capabilities. Outer-planet missions play a key role in NASA's planetary road map, and because communications performance scales inversely as the square of distance, communicating from Pluto or Neptune will be 100 times more difficult than from Mars—and 10 *billion* times more difficult than a typical communications link between a commercial geostationary satellite and the ground! Also, future missions will be more data intensive as we move from an era of flyby missions to long-duration orbiters and in situ investigations, with spacecraft incorporating high-bandwidth instruments such as multispectral imagers.

Based on today's mission operations concept, this increasing mission set cannot be accommodated with the current DSN ground network. A loading study has been performed based on today's mission support scenario of three 8-hour tracking passes per week during cruise and daily 10-hour tracking passes during a prime mission phase (e.g., encounter). Based on these assumptions, even the conservative future mission set leads to a 60 percent oversubscription of DSN antenna capacity by the year 2005.

How will JPL and NASA respond to this challenge? The answer is threefold. First, we will look at the telecommunication link from an end-to-end perspective, starting from the spacecraft instruments all the way through to the project scientists and engineers on the ground. JPL has taken an important step by creating the Telecommunications and Mission Operations Directorate with just this goal in mind. TMOD has the responsibility to define the overall end-to-end architecture for deep-space communications and mission operations and to create a coordinated technology development road map that responds to the needs of the anticipated future mission set. The model of this end-to-end architecture, shown in Fig. 1, is a "solar-system-wide area network" providing seamless connectivity between scientists and their spacecraft instruments. Like the Internet, the solar-system-wide area network provides a layered architecture, with a physical layer embodied by DSN assets on the ground and compatible radio systems on the spacecraft; a data-transport layer with Internet-like protocols, designed to operate efficiently with the long round-trip light times and low signal levels of deep-space links; and an application layer to provide end-to-end information management across the flight–ground system, delivering needed softwore functionality on the ground and on the spacecraft in a migratable, evolvable fashion.

Second, TMOD and its customers will move to a new paradigm in which TMOD provides standard, cost-effective, high-level services. An important example of this is how we think of downlink telemetry. In the past, missions have requested hours of DSN antenna time and dealt with their telemetry at the bit level. In the future, missions will request file transfers, analogous to the file transfer protocol

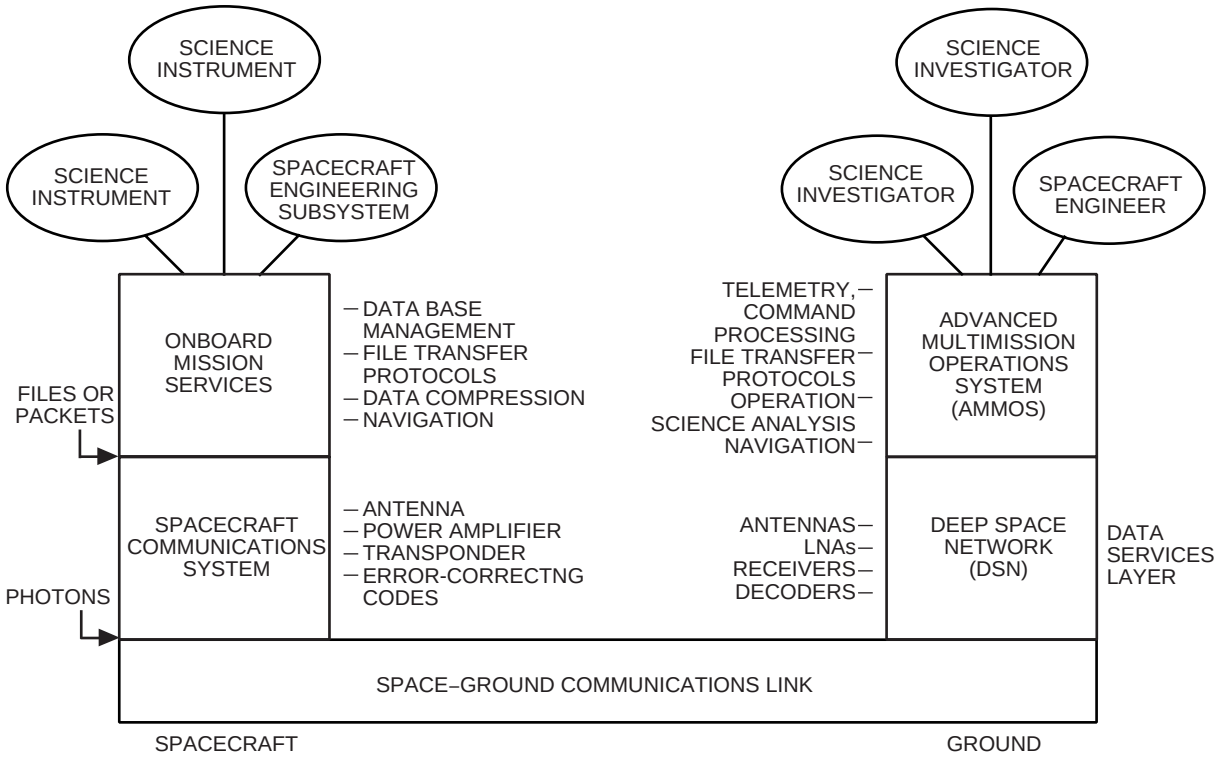

Fig. 1. A layered flight–ground model of deep-space telecommunications and mission operations.

(FTP) services used on the Internet, with robust space communications protocols handling any needed retransmissions, ensuring that all data are successfully delivered to the project. The end-to-end, flight–ground telecommunications system will be engineered to deliver this service reliably and efficiently; for instance, new space link protocols will handle packet acknowledgments and request retransmission of unreceived packets to ensure reliable file transfer without the customer needing to worry about bit-level details.

Third, and perhaps most importantly, rapid infusion of new technology will be key to meeting NASA's deep-space communications challenge. The quantity, quality, and cost of our deep-space communications capabilities are highly dependent on the state of our technology, and advances in component technology will offer opportunities for significant, cost-effective capability growth. Consider this analogy: Every few years, advances in digital-processing technology lead to big performance increases in personal computer modems, allowing one—at low cost—to significantly increase the bandwidth with which one's home computer can interact with the Internet. In a similar way, key technology developments are offering NASA the opportunity to cost effectively increase its deep-space communications capabilities. In particular, Ka-band and optical communications technologies have the potential to provide an order of magnitude increase in performance by the year 2010.

III. Technology Road Map

A. Telecommunications Metrics

To speak quantitatively about communications performance, we first define some useful metrics. In the past, we have tended to think in terms of available antenna hours, and this first metric is easy to understand. To increase this metric, one can build new antennas or increase the utilization of the existing antennas by reducing setup times.

As we move toward a service paradigm, and think in terms of file transfers instead of antenna hours, it is useful to define a second metric representing the data volume that can be downlinked into any given DSN antenna in a given pass length. To be quantitative here, we need to define what is at the other end of the link, and so we will define a "reference spacecraft" at Jupiter distance: We normalize the spacecraft to have an RF output power of 10 W and an antenna effective diameter of 1.0 m (which, for a 50 percent efficient antenna, has a physical diameter of 1.4 m). This is characteristic of the types of communications systems that the mass-, power-, and volume-constrained missions of the future are baselining. To extend this definition to the optical domain, we postulate a spacecraft system consisting of a 30-cm telescope aperture and a 3-W laser output, corresponding to the specifications of the optical transceiver being built within the NASA Deep Space Systems Technology (DSST) Program (also known as the X2000 Technology Program).[3] With this definition, we can speak quantitatively about the data rate that this reference spacecraft can downlink into any given ground antenna (RF) or telescope (optical).

Finally, with this single-aperture definition in place, we define the third metric as the aggregate data-rate capacity for the entire ground network by adding up the downlink rates for all the antennas/telescopes in the DSN. In effect, this corresponds to the aggregate bandwidth that the DSN could supply to an ensemble of reference spacecraft at Jupiter distances in different sky directions. For reference, in terms of this metric, today's DSN provides an aggregate capacity of only 20 kbits per second (kb/s) at S-band (2.3 GHz), 240 kb/s at X-band (8.4 GHz), and no operational capability yet at Ka-band (32 GHz) and optical (1.06 μm).

B. Baseline RF System Improvements

A number of planned improvements are expected to lead to significant improvements in the DSN's current X-band telecommunications capability. These include the following:

(1) *DSN ground station automation:* TMOD is initiating a comprehensive network upgrade that will modernize and simplify DSN subsystems, increase use of standard commercial systems wherever applicable, and significantly increase the level of system operation. In addition to reducing operations costs, this work also will lead to increased antenna utilization due to a reduction in the precalibration/postcalibration time required for each tracking pass, from a current value of over 1 hour down to a goal of 5 minutes. Reducing this precalibration time is especially important as we move toward more short tracking passes. These network improvements are planned to be completed in the 2001 time frame.

(2) *Improved X-band diplexing feed systems:* A new RF feed system design allows diplexed (two-way) communications through a single RF feed without need for a lossy microwave diplexer, resulting in a substantial reduction in the operational system noise temperature.

(3) *Turbo codes:* A new class of error-correcting codes [2] is being developed, offering a 0.8-dB advantage over the current Reed–Solomon/convolutional (15,1/6) concatenated code. NASA's next-generation deep-space transponder, the Spacecraft Transponding Modem, a prototype of which will be completed by 2001, will support this new code, and implementation of turbo decoders in the DSN is planned by 2003.

C. Ka-Band Communications Road Map

The DSN currently supports deep-space communications at S-band (2.3 GHz) and X-band (8.4 GHz). While the baseline RF improvements mentioned above will increase DSN capacity, they are insufficient to meet the anticipated needs of the future mission set. To achieve a more significant increase in deep-space

[3] After this study, DSST Program changes have postponed the development of the optical transceiver, eliminating the option of optical communications for Europa and delaying plans for operational optical capability until the 2008–2010 time frame.

telecommunications capacity, we must either build additional S-/X-band antennas or move to higher communications frequencies [4].

The next frequency allocation for deep-space communications above X-band is Ka-band (32 GHz). Ka-band offers a roughly fourfold performance advantage over X-band for high-rate downlinks, due to the increased directivity of the downlink beam as one moves to shorter wavelengths. This opens up an interesting trade space for future Ka-band missions—with the same antenna size and RF power, and the same amount of tracking time, a Ka-band mission can return four times more data than a comparable X-band mission. Alternatively, total data return can be kept constant while reducing DSN tracking time by a factor of four (an important consideration as we enter an era of full cost accounting in which missions will pay for tracking services). The trade space also includes the spacecraft; instead of increasing data return or reducing tracking time, missions can use the performance gain to reduce spacecraft antenna area or RF power by a factor of four. Each mission will be able to optimize these trades to best benefit from Ka-band's fourfold advantage. For the purpose of this analysis, we make the following assumption: Future missions, starting in 2005, will utilize Ka-band to allow a 50 percent reduction in tracking time while also achieving a factor-of-two increase in overall science data return. In this way, Ka-band provides a win–win solution that copes with the increasing number of missions that the DSN must support while also providing increased science return to each individual mission.

A development road map, including coordinated flight- and ground-technology developments, has been established to support the use of Ka-band in this time frame. Key aspects of this road map, shown in Fig. 2, include the following.

1. Rapid Deployment of Ka-Band Receiving Capabilities in the DSN. DSS 13, the DSN's research and development (R&D) antenna shown in Fig. 3, has served as a test-bed for developing Ka-band ground technologies [3,5,6]. DSS 13 currently supports Ka-band, and the first operational Ka-band capability is just now coming on line at DSS 25, a 34-m beam-waveguide (BWG) antenna at Goldstone's Deep Space Communications Complex. The road map calls for adding Ka-band to all five 34-m BWG antennas by 2003, followed by implementation on the three 34-m high-efficiency (HEF) antennas by 2006, and finally on the three 70-m antennas by 2009. Making the 70-m antennas perform well at the 1-cm wavelength of Ka-band will be technically challenging, as the primary antenna surfaces deform by a significant fraction of this wavelength due to changing gravitational loads as the antennas track targets in elevation angle. The TMOD Technology Program is pursuing two candidate technologies to compensate for these antenna deformations (Fig. 4). In one approach, a small deformable mirror in front of the 70-m RF feed is programmed to compensate for the wavefront distortion caused by the primary surface deformation [10]; this approach can be thought of as the RF equivalent of the adaptive optics systems used in state-of-the-art astronomical telescopes. In the other approach, a cluster of seven feeds collects the defocused Ka-band signal and adaptively recombines it electronically to achieve this compensation [12].

2. Availability of Efficient, Low-Cost, Low-Power, Ka-Band Flight Components. Key elements of the spacecraft radio system include the transponder, the power amplifier, and the high-gain antenna, as discussed below.

(1) The new Small Deep Space Transponder (SDST), developed by Motorola under contract to NASA, is on the New Millennium Deep Space 1 (DS1) Mission. This transponder for the first time provides both X-band and Ka-band downlink exciter options, in addition to its X-band uplink receiving capability. Also, NASA's next-generation deep-space transponder, called the Spacecraft Transponding Modem (STM) and targeted for prototype delivery in 2001 and flight application starting in 2003, will augment the SDST functionality with support of turbo codes, spacecraft timekeeping services, and frame-level interface with the flight computer, all in a smaller, lighter, lower-power, and lower-cost package [11].

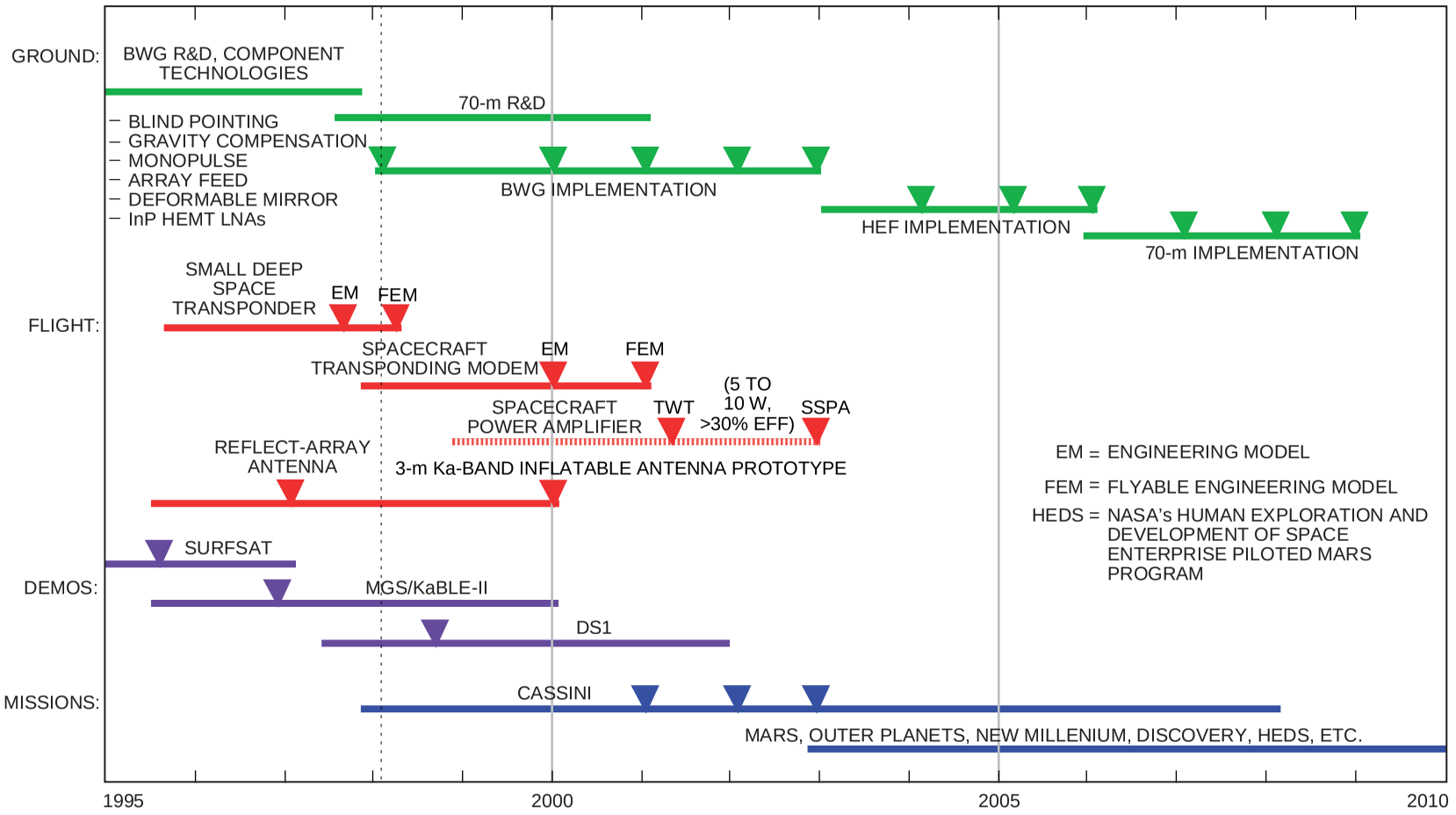

Fig. 2. The Ka-band deep-space telecommunications road map.

Fig. 3. DSS 13, the DSN's 34-m research and development antenna.

(a)

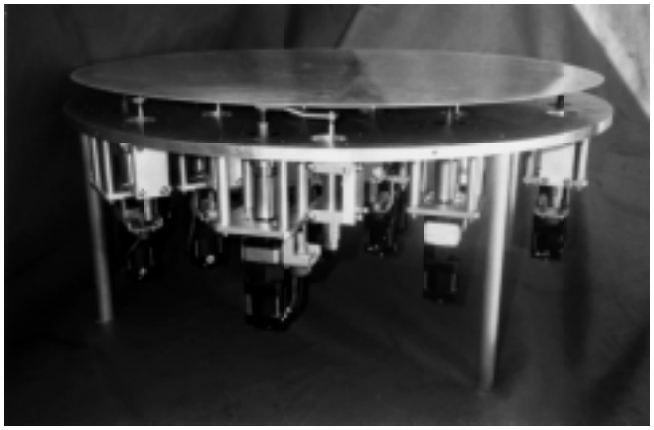

(b)

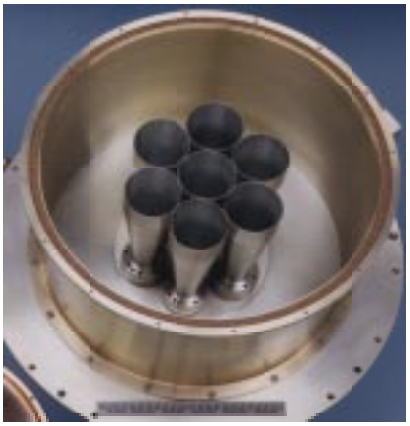

Fig. 4. Two candidate technologies for achieving high aperture efficiency at 32 GHz on the DSN's 70-m antennas: (a) a deformable mirror and (b) a seven-element array feed.

(2) Ka-band power amplifiers are currently a key missing element in the overall Ka-band system. While X-band solid-state power amplifiers (SSPAs) currently offer 30 percent DC-to-RF power efficiency and output power in the 5- to 10-W range, Ka-band SSPAs currently offer only about 10 to 15 percent power efficiency with output power in the 1- to 3-W range. To address this, TMOD currently is establishing plans for the development of a 32-GHz traveling-wave tube amplifier (TWTA), with delivery of a prototype in 2000. Performance goals for this device are 40 percent power efficiency, 10-W RF output, and 1.5-kg total mass. Based on the extensive and highly reliable use of TWTAs in commercial space applications at other microwave frequencies, this appears to be a low-risk path to a near-term Ka-band amplifier with excellent efficiency. Longer-term research on quasi-optic Ka-band SSPA amplifiers is aimed at similar power and efficiency specifications, but at lower mass and cost.

(3) Antennas tend to vary significantly from mission to mission, depending on specific telecommunications needs, spacecraft design issues, and launch vehicle constraints. The Mars Global Surveyor spacecraft is flying a dual-frequency, Cassegrain X-/Ka-band high-gain antenna. Other novel designs with lower mass or stowed volume also are being investigated at Ka-band, including fixed and inflatable reflect-array antennas.

3. Flight Demonstrations. Actual flight demonstrations are critical for validating Ka-band flight and ground components, assessing the increased effects of weather on the Ka-band link, and giving future missions confidence in moving to Ka-band. The Mars Observer spacecraft carried the first deep-space experimental Ka-band downlink in 1992. Initial tests were successful [9], but the loss of the spacecraft limited the experience gained. Subsequently, in 1995, TMOD launched SURFSAT, a student-built payload attached to the upper stage of the RADARSAT launch vehicle, providing X-band (8.4785-GHz), Ku-band (14.148-GHz), and Ka-band (32.0302-GHz) downlink test signals used to validate ground-system technologies. More recently, in 1996, the Mars Global Surveyor spacecraft (Fig. 5) carried a second Ka-band flight experiment that included a 1-W Ka-band SSPA with 11 percent power efficiency and a dual-frequency X-/Ka-band high-gain antenna [1]. The New Millennium DS1 Mission will demonstrate Ka-band downlinks with the Small Deep Space Transponder and a 2.5-W, 15 percent efficient Ka-band SSPA. The flight experiments to date have validated DSN ground-system and spacecraft flight-system performance, as well as atmospheric effects at Ka-band, and the results have been incorporated into the performance predictions presented in the Appendix.

4. Flight Mission Applications. Cassini is the first mission that is flying Ka-band as an operational part of its prime mission. Cassini will use Ka-band uplinks and downlinks, not for telemetry but rather for high-precision radio science experiments. A single Goldstone 34-m BWG antenna, DSS 25, will support these Ka-band links for Cassini, providing a benchmark on ground-station performance and valuable experience in working at Ka-band. A wide array of missions in the 2003-and-beyond time frame are now looking at Ka-band as an option in their mission designs. Potential Ka-band users include missions in the Mars Surveyor Program, the Outer Planets Program (including Europa Orbiter, Pluto Express, and Solar Probe), the new Millennium Program, and the yet-to-be-named missions in the Discovery Program. TMOD will be working with these future missions to cooperatively examine the end-to-end telecommunications link issues and the potential benefits of Ka-band for these missions.

D. Optical Communications Road Map

Looking beyond Ka-band, optical communications holds the promise of even higher telecommunications performance, once again due to much higher directivity of the spacecraft's laser signal toward Earth [4]. (Whereas a 1-m spacecraft RF antenna generates a diffraction-limited beamwidth of about 30 mrad at X-band and 10 mrad at Ka-band, a 10-cm telescope generates an optical beamwidth of 10 μrad or less.) Though in its early stages, the development of optical communications for deep space has already accomplished several important milestones. In 1992, the Galileo Optical Pointing Experiment (GOPEX)

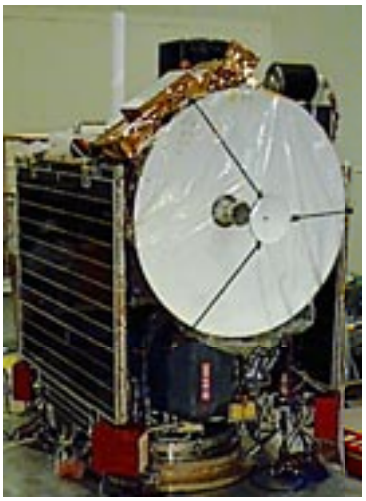

Fig. 5. The Mars Global Surveyor spacecraft, including the Ka-Band Link Experiment (KaBLE-II).

successfully demonstrated transmission of ground-based laser signals up to the Galileo spacecraft [13], and in 1995, JPL and Japan's Communications Research Laboratory collaborated to demonstrate bidirectional optical communications at rates of up to 1 Mb/s between JPL's Table Mountain Facility (TMF), located in Southern California, and the Japanese ETS VI spacecraft (see Fig. 6) [14]. On the flight side, NASA's Crosscutting Technology Program has sponsored the development at JPL of an Optical Communications Demonstrator (OCD), shown in Fig. 7. The OCD is a prototype optical communications terminal applicable to Gb/s near-Earth missions as well as lower-rate deep-space missions [15].

As with the RF domain, TMOD has established a coordinated flight–ground road map of technology development leading to a deep-space optical communications capability, as shown in Fig. 8 and discussed below.

1. Deployment of Optical Ground Stations. In 1998, TMOD initiated the development of an Optical Communications Telescope Laboratory (OCTL), a 1-m optical telescope situated at JPL's Table Mountain Facility. Slated for first light in late 2000, OCTL will serve a role for optical communications very similar to the role played by DSS 13, the DSN's 34-m R&D antenna, in the development of the DSN's emerging Ka-band capabilities. Specifically, it will support early demonstrations of optical communications and also provide a test-bed for component-level developments ultimately needed for operational deep-space optical communications. OCTL will support high slew rates, allowing its use in near-term demonstrations that likely will be conducted from low-Earth-orbiting platforms. In the longer term, operational deep-space optical downlinks will require significantly larger apertures. TMOD's road map calls for the establishment of a network of 10-m optical ground stations for deep-space support in the latter part of the next decade, timed to the need dates of the first deep-space optical links. These nondiffraction-limited ground stations, known as "photon buckets," have lower surface tolerances and, hence, lower costs relative to 10-m-class astronomical telescopes. Each 10-m photon bucket would be augmented with a 1-m uplink telescope, similar to OCTL, which would provide both an uplink communications signal and an uplink reference beacon observed and used by the spacecraft to accurately point the downlink laser signal. Multiple ground stations would be employed to provide site diversity for mitigating the effects of weather on the optical link.

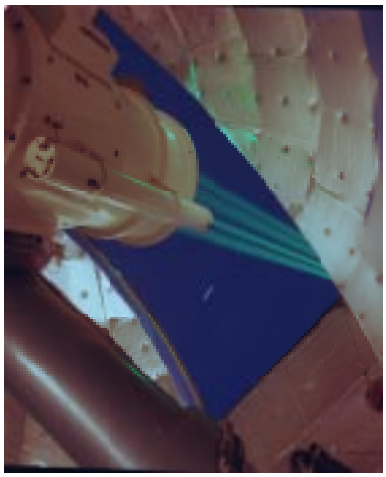

Fig. 6. The multibeam laser uplink from the Table Mountain 0.6-m telescope to the ETS-VI spacecraft during the Gorund-to-Orbit Lasercom Demonstration (GOLD).

Fig. 7. The Optical Communications Demonstrator.

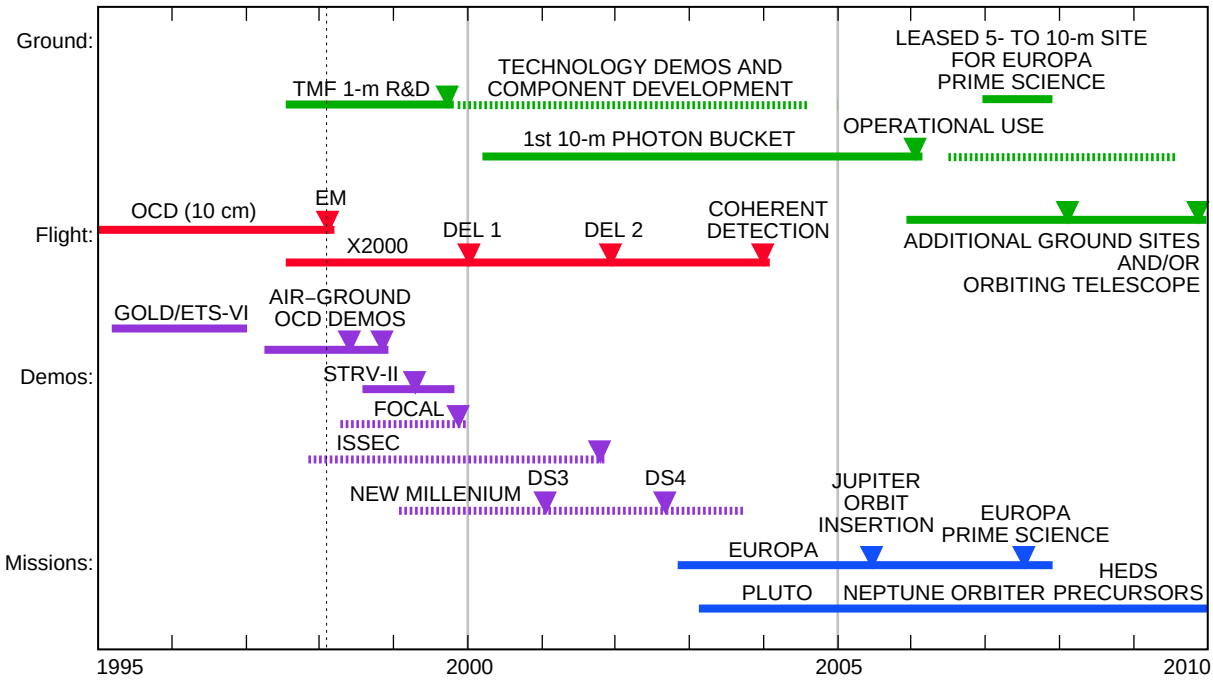

Fig. 8. The optical deep-space telecommunications road map.

2. Development of Optical Flight Components. Building on the successful OCD prototype, NASA recently has embarked on a more ambitious optical transceiver under the X2000 Technology Program at JPL. This effort will lead to a 30-cm-aperture telescope with a 3-W transmitted laser signal, providing uplink (0.53-μm) and downlink (1.06-μm) communications, spatial acquisition and tracking, and two-way ranging functions.

3. Flight Demonstrations. Over the next 2 years, TMOD will carry out ground-to-ground and aircraft-to-ground tests of the OCD at Table Mountain, validating the quantitative performance of the system over extended atmospheric path lengths and testing the spatial acquisition and tracking characteristics of both ends of the link. In the longer term, JPL is exploring the possibility of supporting the Ballistic Missile Defense Organization (BMDO)-sponsored optical communications experiment on Space Technology Research Vehicle (STRV-II) and currently is studying two potential Earth-orbiting demonstrations of the OCD: the Free-Space Optical Communications Assessment Link (FOCAL) Experiment on the Space Transportation System (STS) and the International Space Station as an Engineering Center (ISSEC) Experiment on the International Space Station (ISS). Similarly, NASA's New Millennium Program could provide an ideal platform for flight demonstration, either in the Earth orbiter or deep-space segments of that program. However, a particular concern in the current road map is that none of these opportunities currently is committed. Identifying and committing a flight demonstration of the OCD or the X2000 optical transceiver in the earliest possible time frame is a top priority in technology program planning over the coming year.[4]

4. Flight Mission Applications. The timing of the optical road map, and particularly the implementation of 10-m photon buckets, will be driven by the need dates of the first deep-space users. One aggressive scenario recently examined assumed that the Europa Orbiter Mission (the first launch of the new NASA Outer Planets Program) chooses to fly the X2000-based optical transceiver in order to augment its science return. For one early mission design, the spacecraft would launch in 2003,[5] enter

[4] Ibid.

[5] Ibid.

the Jovian system in 2005, and then spend several years maneuvering into orbit about the moon Europa, culminating in a 30-day prime science mission in 2007. In this scenario, early cruise checkout of the optical flight hardware would be supported by the 1-m OCTL. The first 10-m photon bucket would come on-line in 2006, 1 year prior to the Europa prime science phase. In addition, because of the short nature of that prime phase, NASA would look at the possibility of leasing time on a 5- to 10-m astronomical telescope to augment this first operational site. Based on the success of this first use, NASA then could add additional 10-m ground sites or, alternatively, could assess the cost/benefits of establishing a deep-space optical relay aperture in Earth orbit to get above the detrimental effects of the Earth's atmosphere. Other potential users of optical communications include subsequent Outer Planet Program missions such as Pluto Express and Neptune Orbiter, as well as future Mars relay communications orbiters, providing very high-bandwidth "trunk line" communications back to Earth for sophisticated robotic surface rovers and aerobots, and eventually for piloted Mars missions.

IV. Conclusion

The impact of these new technologies can be quantified by revisiting the telecommunications metrics we defined in Section III.A. First is the simple metric of available DSN tracking time and the anticipated 60 percent DSN oversubscription based on a projection of the needs of the rapidly expanding mission set and using current operations concepts. The Ka-band road map, coupled with planned ground-system automation (to increase antenna availability) provides a cost-effective path to deal with this demand while simultaneously providing increased science data return to future missions. With network-wide Ka-band support on all 34-m BWG antennas by 2003 and the availability of efficient, low-mass, low-cost Ka-band flight components in this same time frame, Ka-band will be a very viable option for missions in the 2003 to 2005 time frame and beyond. With the roughly fourfold performance advantage of Ka-band relative to X-band, future missions will be able to adopt a new operations concept that requires a factor of two less DSN tracking time but still provides roughly a factor of two more data volume. In addition, implementation of highly automated DSN ground systems in this time frame will increase available antenna hours by reducing precalibration/postcalibration time. A revised DSN loading study, based on the assumption that NASA missions starting in 2005 will use Ka-band to reduce their tracking requirements to one 5-hour pass per week in cruise phase and one 5-hour pass per day in the prime science phase (which still provides an overall increase in data volume return), shows that the anticipated mission set can be well supported with existing DSN assets outfitted with new Ka-band electronics.

Moving to our second metric, the actual data volume that can be obtained in one of these short, 5-hour tracking passes is of interest to future mission designers. Link analyses for X-band, Ka-band, and optical links using various ground assets exhibit the performance gains possible by moving to higher frequencies, as shown in Table 1. (These links represent theoretical upper limits [see the Appendix] and do not include additional link margins, the allocation of power to residual carriers or ranging channels, etc.; see the table notes for detailed assumptions. Use these numbers as a guide to the *relative* performance of different configurations.) Several observations can be made: First, these numbers confirm that a 34-m antenna Ka-band link is roughly comparable to a 70-m antenna X-band link and nearly four times higher than a 34-m antenna X-band link. Second, if the development of adaptive Ka-band feed systems succeeds on the 70-m antennas, even higher performance is possible. In fact, the Ka-band 70-m antenna link provides performance nearly equivalent to the optical 10-m telescope link for the spacecraft configurations considered here.

Finally, we can look at our third metric, aggregate ground network capacity for deep-space communications, to view at the highest level how these technology developments will lead to a dramatic increase in the bandwidth available for supporting fleets of robotic and, ultimately, piloted missions in the new millennium. Figure 9 shows the growth of this aggregate communications data-rate capacity metric at S-band, X-band, Ka-band (see the Appendix), and optical frequencies between now and 2010, based on the technology road maps presented here. Again, several observations can be made: First, the use of

Table 1. Data return (Mbytes) for a 5-hour tracking pass.

Planet	X-band		Ka-band		Optical	
	34-m antenna, Mbytes	70-m antenna, Mbytes	34-m antenna, Mbytes	70-m antenna, Mbytes	1-m telescope, Mbytes	10-m telescope, Mbytes
Mars	182.6	727.5	659.6	1772.1	29.5	2151.3
Jupiter	42.2	168.2	152.5	409.6	6.8	497.3
Saturn	12.5	49.9	45.2	121.4	2.0	147.4
Pluto	0.7	2.9	2.6	7.1	0.1	8.4

Notes:
(1) RF cases referenced to a 1-m diameter effective spacecraft antenna, 10-W RF radiated power.
(2) Optical cases referenced to a 30-cm spacecraft telescope, 3-W optical transmitted power, $l = 1.06$ m.
(3) RF values averaged over complexes; optical assumes Goldstone.
(4) RF cases assume 6-K closed-cycle refrigerator (CCR), high-electron-mobility transistor (HEMT), low-noise amplifier (LNA) systems.
(5) Optical cases averaged over the Sun–Earth–probe (SEP) angle.
(6) Optical performance varies with SEP angle; 10 m: ±50 percent (1 m: ±5 percent) for SEP = 180 deg to 10 deg.
(7) All cases referenced to a data rate at a 30-deg elevation angle.
(8) RF links assume 90 percent availability; optical assumes 70 percent; data volume deweighted by availability.
(9) No additional link margin included.

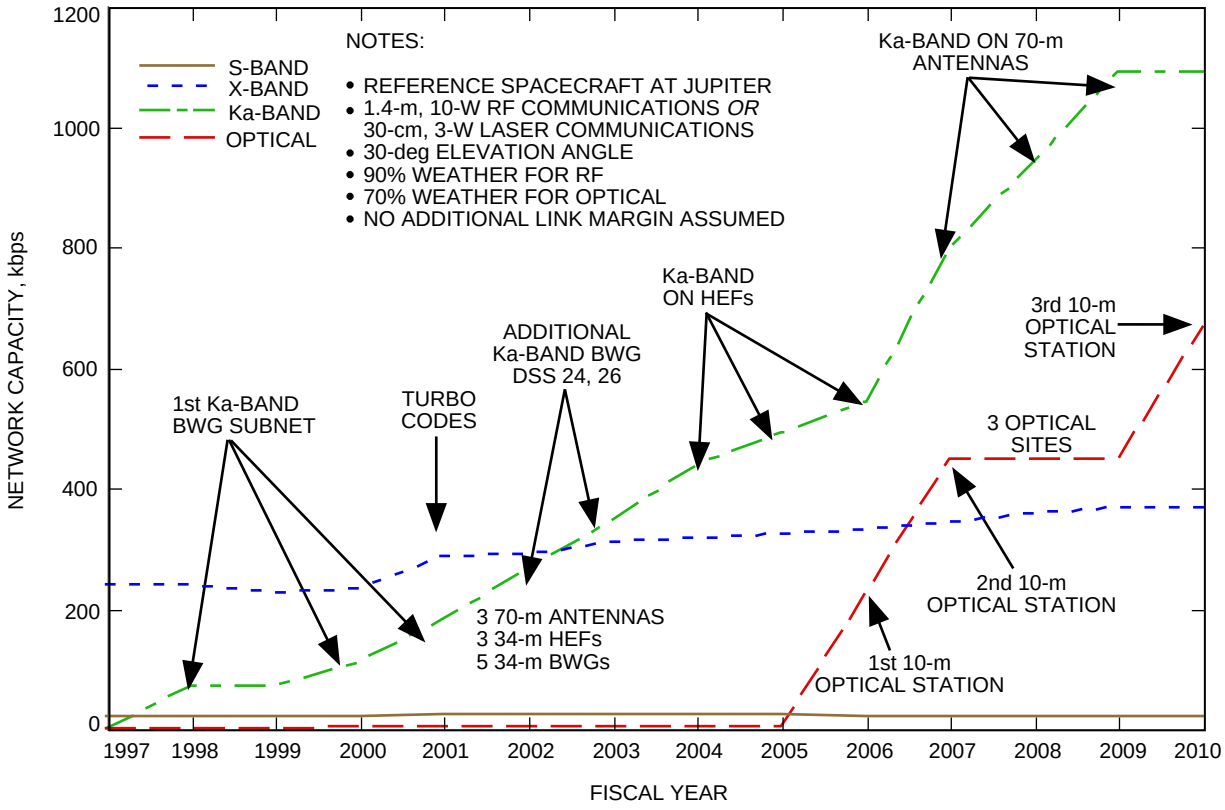

Fig. 9. The projected growth in NASA's deep-space communications capability based on new RF and optical communications technologies.

new turbo codes as well as planned improvements in our current feed systems will lead to continuous incremental growth of our existing X-band capability. Second, the proposed Ka-band implementations provide much more dramatic growth. The Ka-band capability of just the five BWG antennas will outperform the entire DSN at X-band, and with the addition of Ka-band to the HEF and 70-m antennas, the resulting Ka-band capability will be more than four times our current X-band capacity. Finally, optical communications provides a long-range path to future growth. The first optical 10-m station will offer roughly the performance of today's entire DSN capacity.

In conclusion, new RF and optical technologies are poised to provide breakthrough increases in NASA deep-space telecommunications capacity, allowing NASA to meet the needs of a growing and increasingly challenging mission set while offering increased data return to individual missions. In the near term, the addition of Ka-band capabilities to existing DSN antennas is an extremely cost-effective way to increase capacity. In the longer term, optical communications appears to be a promising path for future growth. Achieving this growth will require a coordinated approach toward the development of flight and ground technologies. Critical items on the road maps include developing efficient Ka-band spacecraft amplifiers, demonstrating the potential performance of the 70-m antennas at Ka-band, and establishing one or more near-term optical flight demonstrations. The road map presented here provides a cost-effective path to significant improvements in NASA's deep-space communications capability, moving toward NASA's ultimate goal of establishing a virtual presence throughout the solar system.

Acknowledgments

The work reported here reflects contributions from many people at JPL. The authors especially thank Gael Squibb, Rich Miller, Steve Townes, Jim Layland, Jeff Osman, Chris Yung, Mark Gatti, Jim Lesh, Keith Wilson, Hamid Hemmati, David Rochblatt, Javier Bautista, Sam Petty, Bob Clauss, Steve Slobin, Shervin Shambayati, Fabrizio Pollara, and Anil Kantak for valuable input and discussions in developing this road map.

References

[1] S. Butman, D. Morabito, A. Mittskus, J. Border, J. Berner, C. Whetsel, M. Gatti, C. Foster, V. Vilnrotter, H. Cooper, A. Del Castillo, A. Kwok, J. Weese, M. Speranza, R. Davis, W. Adams, A. McMechen, C. Goodson, G. Bury, and D. Recce, "The Mars Global Surveyor Ka-Band Link Experiment (MGS/KaBLE-II)," *Proceedings of the Third Ka-Band Utilization Conference*, Sorrento, Italy, pp. 179–186, September 15–18, 1997.

[2] D. Divsalar and F. Pollara, "On the Design of Turbo Codes," *The Telecommunications and Data Acquisition Progress Report 42-123, July–September 1995*, Jet Propulsion Laboratory, Pasadena, California, pp. 99–121, November 15, 1995. http://tmo.jpl.nasa.gov/tmo/progress_report/42-123/123D.pdf

[3] C. Edwards, L. Deutsch, M. Gatti, J. Layland, J. Perret, and C. Stelzried, "The Status of Ka-band Communications for Future Deep Space Missions," *Proceedings of the Third Ka-Band Utilization Conference*, Sorrento, Italy, pp. 219–225, September 15–18, 1997.

[4] H. Hemmati, K. Wilson, M. K. Sue, L. J. Harcke, M. Wilhelm, C.-C. Chen, J. R. Lesh, Y. Feria, D. Rascoe, F. Lansing, and J. W. Layland, "Comparative Study of Optical and Radio-Frequency Communication Systems for a Deep-Space Mission," *The Telecommunications and Data Acquisition Progress Report 42-128, October–December 1996*, Jet Propulsion Laboratory, Pasadena, California, pp. 1–33, February 15, 1997.
http://tmo.jpl.nasa.gov/tmo/progress_report/42-128/128N.pdf

[5] V. Y. Lo, "Ka-Band Monopulse Antenna-Pointing Systems Analysis and Simulation," *The Telecommunications and Data Acquisition Progress Report 42-124, October–December 1995*, Jet Propulsion Laboratory, Pasadena, California, pp. 104–112, February 15, 1996.
http://tmo.jpl.nasa.gov/tmo/progress_report/42-124/124F.pdf

[6] D. D. Morabito, "The Efficiency Characterization of the DSS-13 34-Meter Beam-Waveguide Antenna at Ka-Band (32.0 and 33.7 GHz) and X-Band (8.4 GHz)," *The Telecommunications and Data Acquisition Progress Report 42-125, January–March 1996*, Jet Propulsion Laboratory, Pasadena, California, pp. 1–20, May 15, 1996.
http://tmo.jpl.nasa.gov/tmo/progress_report/42-125/125D.pdf

[7] National Aeronautics and Space Administration, *NASA Strategic Plan*, NASA Policy Directive (NPD)-1000.1, Washington, DC, 1998.

[8] National Research Council, Committee on Advanced Space Technology, Aeronautics and Space Engineering Board, Commission on Engineering and Technical Systems, *Space Technology for the New Century*, Washington, DC: National Academy Press, 1998.

[9] T. A. Rebold, A. Kwok, G. E. Wood, and S. Butman, "The Mars Observer Ka-band Link Experiment," *The Telecommunications and Data Acquisition Progress Report 42-117, January–March 1994*, Jet Propulsion Laboratory, Pasadena, California, pp. 250–282, May 15, 1994.
http://tmo.jpl.nasa.gov/tmo/progress_report/42-117/117u.pdf

[10] S. R. Rengarajan, W. A. Imbriale, and P. W. Cramer, "Design of a Deformed Flat Plate to Compensate the Gain Loss Due to the Gravity-Induced Surface Distortion of Large Reflector Antennas," URSI Commission B 1998 Electromagnetic Theory Symposium, Thessaloniki, Greece, May 25–28, 1998.

[11] A. L. Riley, S. Kayalar, A. Mittskus, D. Antsos, E. Grigorian, E. Olson, J. Neal, E. Satorius, and A. Kermode, "New Millennium Deep Space Tiny Transmitter: First Phase of a Digital Transponder," *Proceedings of the AIAA/IEEE Digital Avionics Systems Conference*, Atlanta, Georgia, pp. 225–230, October 27–31, 1996.

[12] V. Vilnrotter and B. Iijima, "Analysis of Array Feed Combining Performance Using Recorded Data," *The Telecommunications and Data Acquisition Progress Report 42-125, January–March 1996*, Jet Propulsion Laboratory, Pasadena, California, pp. 1–13, May 15, 1996.
http://tmo.jpl.nasa.gov/tmo/progress_report/42-125/125C.pdf

[13] K. E. Wilson and J. R. Lesh, "An Overview of the Galileo Optical Experiment (GOPEX)," *The Telecommunications and Data Acquisition Progress Report 42-114, April–June 1993*, Jet Propulsion Laboratory, Pasadena, California, pp. 192–204, August 15, 1993.
http://tmo.jpl.nasa.gov/tmo/progress_report/42-114/114Q.pdf

[14] K. E. Wilson, J. R. Lesh, K. Araki, and Y. Arimoto, "Overview of the Ground-to-Orbit Lasercom Demo," Free-Space Laser Communication Technologies IX, *Proceedings of SPIE*, vol. 2990, San Jose, California, pp. 23–30, February 13–14, 1997.

[15] T.-Y. Yan, M. Jeganathan, and J. Lesh, "Progress on the Development of the Optical Communications Demonstrator," Free-Space Laser Communication Technologies IX, *Proceedings of SPIE*, vol. 2990, San Jose, California, p. 94, February 13–14, 1997.

Appendix

1998 and Future DSN RF Aggregate Data Rate Capacities

C. Stelzried[1]

I. Analysis

For a spacecraft-to-ground data RF link, the maximum data rate [A-1], R_{max}, is increased at higher frequencies (shorter wavelengths) primarily by the more focused downlink transmitted signal beam (higher G_t) and is given by

$$R_{max}\ (\text{b/s}) = P_t G_t \frac{\dfrac{A_r}{T_{op}}}{4\pi k L D^2 \dfrac{E_b}{N_o}} \tag{A-1a}$$

For calculation convenience, using the defined DSN conventional ground receiving system G/T figure of merit, this can be written as

$$R_{max}\ (\text{b/s}) = P_t A_t \frac{\dfrac{G_r}{T_{op}}}{4\pi k L D^2 \dfrac{E_b}{N_o}} \tag{A-1b}$$

where

[1] TMOD Technology Program Office.

$\frac{A_r}{T_{op}} =$ ground receiving system figure of merit, m^2/K

$\frac{G}{T} = \frac{G_r}{T_{op}} =$ ground receiving system performance figure of merit, 1/K

$G = G_r = \frac{4\pi A_r}{\lambda^2} =$ ground receiving antenna effective gain, ratio

$G_t = 4\pi\frac{A_t}{\lambda^2} =$ spacecraft downlink effective antenna gain, ratio

$A = A_r =$ ground receiving antenna effective area, m^2

$A_t =$ spacecraft downlink effective antenna area, m^2

$T_{op} =$ ground system operating noise temperature, K

$P_t =$ spacecraft transmitted power, W

$k =$ Boltzmann's constant $= 1.3807 \times 10^{-23}$ J/K

$L =$ overall loss $= L_{tr}L_mL_s$, ratio ≥ 1 or $= 1$

$L_{tr} =$ spacecraft transmitter-to-ground receiving system losses, such as mispointing and polarization, ratio

$L_m =$ modulation loss $= \frac{P_r}{S} = \left(\frac{1}{\sin\theta}\right)^2$, ratio

$L_s =$ receiving system losses, ratio

$\theta =$ modulation phase angle, deg

$S =$ portion of the received signal power in the data modulation sidebands $= \frac{P_r}{L_m}$, W

$Pr =$ ground system received power, W

$D =$ distance between the spacecraft and ground antennas, m

$\lambda =$ carrier wavelength, m

$\frac{E_b}{N_o} =$ threshold signal energy per bit per noise power density, ratio

II. DSN Current 1998 System Parameters, Analysis, and Antenna Data Rates, and Baseline RF Aggregate Data Rate Capacity Results

Equation (A-1) is used to compute the data rates for each DSN antenna with the assumptions of the DSN aggregate data rate capacity as defined in Section 3.A. These data rates are summed to result in the DSN aggregate data rate capacity performance. Spacecraft mispointing losses are accounted for assuming an antenna mispointing of 0.1 deg and a Gaussian shaped beam. Similarly, the ground antenna pointing losses are accounted for assuming S- and X-band pointing offsets of 3 mdeg for the 70-m antennas and 4 mdeg for all the others and assuming Ka-band pointing offsets of 0.3 mdeg for all of the antennas. It is assumed that active feedback pointing systems such as conscan and/or monopulse techniques will be used to achieve or improve these DSN antenna-pointing capabilities.

The data link coding parameter, E_b/N_o, varies with the mission and the latest implementation in the DSN and is continually improved, as shown in Table A-1.[2] For the 1990 to 2000 time period, the

[2] S. Shambayati, private communication, Jet Propulsion Laboratory, Pasadena, California, December 2, 1997.

Table A-1. DSN decoding capability versus date, assuming a 10^{-5} BER.

Code	E_b/N_o, dB	Decoding	Mission (time period)
(32,1/2)[a]	7.1	Sequential	Pioneers 10/11 (1972–1974)
Reed–Mueller (32,6)	6.0	Block decoding	Vikings 1/2 (1975–1976)
(7,1/2),[a] Reed–Solomon(255,223)	2.4	Concatenated[b]	Voyagers (1977–1989)
(15,1/6),[a] Reed-Solomon(255,223)	0.6	Concatenated[b]	Cassini (1990–2000)
Turbo codes	−0.2	Turbo decoding	(2001–beyond)

[a] Convolutional code.

[b] Concatenated Viterbi and Reed–Solomon decoding.

best (lowest E_b/N_o) available performance uses a concatenated convolutional (15,1/6) and Reed–Solomon (225,223) code. This code was available for Galileo, was used by Mars Pathfinder, and is available for the Cassini missions with an E_b/N_o performance of 0.6 dB for a bit error rate (BER) of 10^{-5}.

The current (1998) values of T_{op} and G_r (tabulated as antenna efficiency $= A_e/A_p$, where $A_e =$ antenna effective area, as defined by $G_r = 4\pi A_e/\lambda^2$ and $A_p =$ physical area, and assuming S-band = 2.295 Ghz and X-band = 8.42 GHz) for the various DSN antennas are obtained from a DSN internal document.[3] These are tabulated in Table A-2 for a 30-deg antenna elevation angle and 90 percent weather (the system noise temperature, based on long-term data collection, is equal to or less than the specified value 90 percent of the time). The averaged data rate is reduced by 10 percent to account for the 90 percent weather. A coding parameter value of 0.6 dB was used. This analysis results in 1998 DSN RF aggregate data-rate values of 20.1 and 239.3 kb/s for S- and X-bands being used as the baseline for comparison with the road map future improvements study.

III. DSN Future System Parameters, Analysis, and Antenna Data Rates, and RF Aggregate Data Rate Capacity Results

Improvements continue to be made in DSN X-band antenna efficiencies and low noise amplifier (LNA) noise temperatures. In addition, Ka-band capabilities are being advanced and have been verified at DSS 13 with the student-built SURFSAT, the Mars Observer (MO), and the Mars Global Surveyor (MGS) missions as well as with the Goldstone DSS-25 BWG antenna's first DSN usage for a radio science Cassini mission application. The estimated RF vacuum parameter performances (not accounting for the atmosphere but including antenna mispointing and assuming a 30-deg antenna elevation angle) for antenna efficiencies and system noise temperatures (assuming HEMT LNAs) with the resultant G/T values are as shown in Table A-3. These vacuum estimates are important for comparison with actual future X- and Ka-band antenna and LNA hardware parameter performance development and deployment in the field and are used to define implementation system requirements.

Accounting for the atmosphere, assuming current DSN estimates[4] and a coding parameter value of −0.2 dB, results in future DSN RF data rates of 374.3 and 1088.3 kb/s for X- and Ka-bands, as shown in

[3] *Deep Space Network/Flight Project Interface Design Handbook, Volume 1: Existing DSN Capabilities*, JPL 810-5, Rev. D (internal document), Jet Propulsion Laboratory, Pasadena, California, 1976. (DSN antenna parameter values also are available from Web site http://deepspace1.jpl.nasa.gov/810-5/.)

[4] Ibid.

Table A-4. These data rates are converted to Mbytes of data collected during a 5 hour pass by multiplying by the factor (5 hours × (3600 s/h)/8000 kb) to provide the RF data return values at Jupiter shown in Table 1. The aggregate DSN capacity data rates are estimated to be increased by about 1 dB using LNA masers instead of HEMTs.

Table A-2. DSN 1998 S- and X-band antenna efficiencies and system noise temperatures, T_{op}, for antennas at 30-deg elevation angles and 90 percent weather, with the resulting baseline RF aggregate capacity data-rate values.

Location	DSS	Diameter, m	Antenna efficiency,[a] ratio		System noise temperature, K		Data rate, kb/s	
			S-band	X-band	S-band	X-band	S-band	X-band
Standard antennas								
Australia	42	34	0.601	0.438	32.6	33.4	0.72	6.84
Spain	61	34	0.601	0.438	32.6	33.4	0.72	6.84
High-efficiency antennas								
Goldstone	15	34	0.586	0.701	42.7	32	0.54	11.4
Australia	45	34	0.586	0.695	43	34.3	0.53	10.6
Spain	65	34	0.586	0.695	49	34.3	0.47	10.6
70-m antennas								
Goldstone	14	70	0.738	0.647	22.3	25.8	5.49	55.5
Australia	43	70	0.737	0.62	23.1	28.1	5.30	48.9
Spain	63	70	0.737	0.644	24.4	28.1	5.02	50.8
Beam-waveguide antennas								
Goldstone	24	34	0.671	0.688	39.7	28.4	0.66	12.7
Goldstone	25	34	—[b]	0.689	—[b]	38.4	—[b]	9.38
Australia	34	34	0.679	0.658	39.1	46.9	0.68	7.33
Spain	54	34	—[b]	0.658	—[b]	40.6	—[b]	8.46
Aggregate DSN data rate							20.1	239.3

[a] Includes diplexer, antenna mispointing, and atmospheric losses.

[b] No S-band capability.

Table A-3. DSN estimated future X- and Ka-band antenna efficiencies and system noise temperatures, T_{op}, for antennas at 30-deg elevation angles in a vacuum (accounting for antenna mispointing), with the resulting RF hardware G/T performance estimates.

Location	DSS	Diameter, m	Antenna efficiency, ratio		System noise temperature, K		G/T, dB	
			X-band	Ka-band	X-band	Ka-band	X-band	Ka-band
High-efficiency antennas								
Goldstone	15	34	0.771	0.642	17.0	27.5	56.1	64.8
Australia	45	34	0.771	0.642	17.0	27.5	56.1	64.8
Spain	65	34	0.771	0.642	17.0	27.5	56.1	64.8
70-m antennas								
Goldstone	14	70	0.682	0.425	17.0	27.5	61.9	69.3
Australia	43	70	0.682	0.425	17.0	27.5	61.9	69.3
Spain	63	70	0.682	0.425	17.0	27.5	61.9	69.3
Beam-waveguide antennas								
Goldstone	24	34	0.752	0.615	19.5	29.5	55.4	64.3
Goldstone	25	34	0.752	0.615	19.5	29.5	55.4	64.3
Goldstone	26	34	0.752	0.615	19.5	29.5	55.4	64.3
Australia	34	34	0.752	0.615	19.5	29.5	55.4	64.3
Spain	54	34	0.752	0.615	19.5	29.5	55.4	64.3

Table A-4. DSN future X- and Ka-band antenna efficiencies and system noise temperatures, T_{op}, for antennas at 30-deg elevation angles and 90 percent weather, with the resulting RF aggregate capacity data-rate values.[a]

Location	DSS	Diameter, m	Antenna efficiency, ratio		System noise temperature, K		Data rate, kb/s	
			X-band	Ka-band	X-band	Ka-band	X-band	Ka-band
High-efficiency antennas								
Goldstone	15	34	0.757	0.585	22.2	52.3	21.4	90.3
Australia	45	34	0.751	0.520	24.5	80.5	19.2	52.1
Spain	65	34	0.751	0.520	24.5	80.5	19.2	52.1
70-m antennas								
Goldstone	14	70	0.669	0.388	22.2	52.3	80.1	253.5
Australia	43	70	0.663	0.344	24.5	80.5	72.1	146.3
Spain	63	70	0.663	0.344	24.5	80.5	72.1	146.3
Beam-waveguide antennas								
Goldstone	24	34	0.737	0.561	24.7	54.3	18.7	83.4
Goldstone	25	34	0.737	0.561	24.7	54.3	18.7	83.4
Goldstone	26	34	0.737	0.561	24.7	54.3	18.7	83.4
Australia	34	34	0.731	0.498	27.0	82.5	17.0	48.7
Spain	54	34	0.731	0.498	27.0	82.5	17.0	48.7
Aggregate DSN data rate							374.3	1088.3

[a] Includes pointing and atmospheric losses (assumes X- and Ka-band diplexed feeds).

Acknowledgments

Many thanks are due to the contributors, who include S. Slobin D. Rochblatt, S. Petty, S. Shambayati, and R. Clauss for the atmosphere, antenna, LNA, coding performance, and system values used for this analysis.

Reference

[A-1] N. A. Renzetti, C. T. Stelzried, G. K. Noreen, S. D. Slobin, S. M. Petty, D. L. Trowbridge, H. Donnelly, P. W. Kinman, J. W. Armstrong, N. A. Burow, M. K. Tam, J. W. Layland, and A. L. Berman, *The Deep Space Network—A Radio Communications Instrument for Deep Space Exploration*, JPL Publication 82-104, Jet Propulsion Laboratory, Pasadena, California, pp. 2–6, Eqs. 2–9, July 15, 1983.